J Appl Electrochem (2007) 37:1099–1106
DOI 10.1007/s10800-007-9362-9

ORIGINAL PAPER

Electrochemical behavior of aluminum bronze in sulfate-chloride media

Waheed A. Badawy · Rabab M. El-Sherif · Hassan Shehata

Received: 21 November 2006 / Revised: 2 July 2007 / Accepted: 2 July 2007 / Published online: 20 July 2007

Abstract The electrochemical behavior, especially the corrosion and passivation, of a Cu–Al bronze was investigated. Conventional electrochemical techniques including open-circuit potential, anodic polarization, cyclic voltammetry and electrochemical impedance spectroscopy were used. It was found that the addition of chloride ion up to 0.15 M in 0.5 M Na_2SO_4 solution decreases the corrosion rate due to the formation of CuCl, whereas at higher concentration of the chloride ion, the corrosion rate increases due to the formation of the soluble $CuCl_2^-$. The activation energy was found to be 10 kJ mol^{-1}. This value indicates that the corrosion process is under diffusion control. The impedance measurements showed that the passive film can be represented by a duplex layer, a relatively thick porous outer film on top of a thin compact layer. An equivalent circuit was used to explain and analyze the impedance data. The model includes another R-C combination and Warburg impedance in addition to the simple Randles cell to account for the spontaneously formed passive film and the diffusion phenomena.

Keywords Aluminium bronze · Corrosion · Chloride · Cyclic voltammetry · Impedance · Sulfate

W. A. Badawy (✉) · R. M. El-Sherif
Chemistry Department, Faculty of Science,
University of Cairo, Cairo, Egypt
e-mail: wbadawy@chem-sci.cu.edu.eg;
wbadawy@wbadawy.csc.org.eg

H. Shehata
EMISAL Company, Fayoum, Egypt

1 Introduction

Copper-based alloys are among the most important metals used in marine environments, due to their excellent electrical and thermal conductivity, good corrosion resistance and ease of manufacture [1–3]. Therefore, copper-alloys have wide industrial applications as condensers and heat-exchanger systems in saline water [4]. Aluminum–bronze is widely used in heat-exchangers. The addition of aluminum to copper increases its corrosion resistance in sea water, sulphuric acid and salt solutions [5]. Alloys with aluminum content up to 8% have completely face-centered cubic (fcc) α structures and good mechanical and corrosion resistance. The corrosion resistance of both aluminum bronze and nickel aluminum bronze has been attributed to a sustainable protective layer of alumina (Al_2O_3) which forms quickly on the alloy surface post-exposure to the corrosion environment [6, 7]. For Cu–Al alloys, passivation is based on aluminum which has a greater affinity to O_2 than copper, forming Al_2O_3 [8]. The cathodic and anodic polarization of nickel aluminum bronze was investigated in seawater [2, 5]. The results indicated that, the reduction of oxygen dominates the cathodic process and is controlled by the exchange of a single electron. This behavior is similar to that of pure copper. In the anodic process the chloride ion facilitates selective dissolution of copper and the process is under a form of mixed mass and charge transfer. The structure of the protective layer of copper alloys is generally ascribed to an outer $CuO/Cu(OH)_2$ and an inner Cu_2O layer [9]. The later was reported to be responsible for the corrosion inhibition of the alloy when exposed to aggressive media [3, 4]. The protective action of the passive film seems to be dependent on good adherence to the metal and high receptivity towards electronic and ionic conductance. In a series of publications the optimum ratio of the sulfate/

chloride introduced to the production plant in order to minimize the corrosion rate of 304 L steel was investigated [10–12]. The introduction of Al–bronze in the production line of Na_2SO_4 makes the investigation of the electrochemical behavior of this alloy in the industrial electrolyte mixture and the cooling water system an important problem worthy of detailed investigation. The aim of this work is to investigate the corrosion behavior of the Cu–Al–As alloy cut from the heat exchanger operated in the extraction of Na_2SO_4 by EMISAL Company from Lake Quaron. It is aimed at the optimization of production conditions, especially the sulfate/chloride ratios introduced to the plant in order to minimize the rate of corrosion of the alloy and to increase the life time of the heat exchangers.

2 Experimental

The working electrodes were made from Cu–Al alloy samples cut from heat exchanger tubes used in the production of sodium sulfate from Lake Quaroun, Fayoum, Egypt. The mass spectroscopic analysis of this material is presented in Table 1. The test electrodes were mounted into glass tubes using a two-component epoxy resin leaving a surface area of 0.08 cm^2 to contact the solution. The cell was a conventional three-electrode all glass cell with a platinum counter electrode and Ag/AgCl reference electrode [E^o = 0.197 V (NHE)]. Before each experiment the working electrode was polished mechanically using successive grades of emery paper up to 1,000 grit and then with alumina (1 μm). The electrode was then rubbed with a smooth polishing cloth washed with triple distilled water and transferred quickly to the cell. The test solutions were prepared from analytical grade reagents and triply distilled water. The test solution was adjusted to pH 7 by small additions of NaOH and H_2SO_4 and then checked by a pH meter. Potentiodynamic polarization experiments were conducted using a potentiostat/galvanostat at a scan rate of 1 mV s^{-1}. The use of low scan rate was found to give more reliable results because it permits conditions nearer to the steady state [8]. All cyclic voltammetry measurements were carried out using a scan rate 5 mV s^{-1}. The electrochemical impedance investigations were performed using a Zahner Elektrik IM6 electrochemical workstation. The amplitude of the superimposed AC-signal was 10 mV peak to peak. The method involves direct measurements of the impedance Z and the phase shift θ of the electrochemical system in the frequency range 0.1–10^5 Hz. To achieve reproducibility, each experiment was carried out at least twice. In some cases multiple repetitions were carried out until reproducible data were obtained. All experiments were carried out at room temperature, 25 ± 1 °C, and the potentials were measured against and referred to the Ag/AgCl electrode. The experimental details are as described elsewhere [3, 4].

Table 1 Mass spectroscopic analysis of the aluminum bronze

Element	Percentage
Al	6.11
As	0.03
Cu	93.80
Fe	0.019
Pb	0.002

3 Results and discussion

3.1 Open-circuit potential measurements

The open-circuit potential of the Cu–Al alloy was followed over a period of 1 h in 0.5 M Na_2SO_4 solution containing different chloride ion concentrations [0–0.5 M Cl^-] and the results are presented in Fig. 1. Generally the steady state potential was reached within 15 min from the electrode immersion in the test solution; the addition of chloride ions shifts the potential towards more negative value and the negative shift increases as the concentration of chloride ions increases. This negative shift can be attributed to the selective leaching of the active components from the alloy surface [13].

3.2 Potentiodynamic measurements

3.2.1 Corrosion measurements

The effect of chloride ion concentration [0–0.5 M] on the potentiodynamic polarization behavior of the Cu–Al alloy

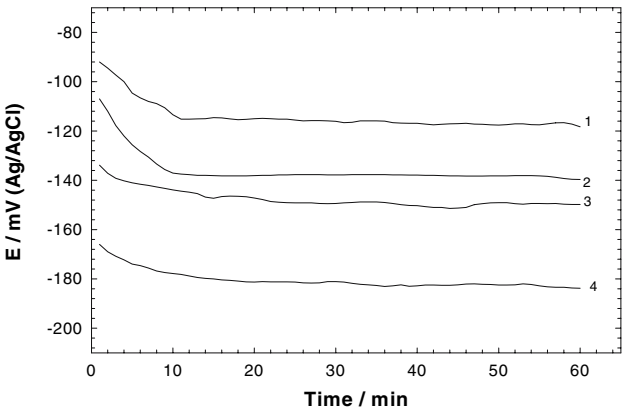

Fig. 1 Variation of the open-circuit potential for Cu–Al alloy with time in neutral 0.5 M Na_2SO_4 solution containing different chloride ion concentrations at 25 °C:[Cl^-]:1 = 0.0 M, 2 = 0.1 M, 3 = 0.2 M, 4 = 0.5 M

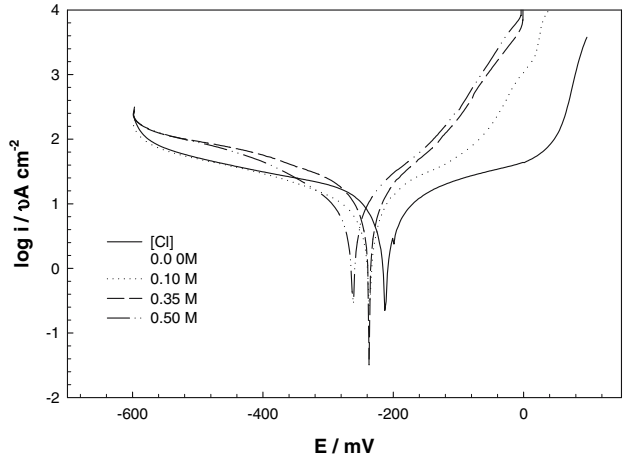

Fig. 2 Typical Tafel plots for Cu–Al alloy in neutral 0.5 M Na_2SO_4 solution as a function of chloride ion concentrations at 25 °C

in 0.5 M Na_2SO_4 at pH 7 is presented in Fig. 2. The cathodic branch of the curves represents the oxygen reduction, while the anodic one shows copper dissolution [14]. However, in aqueous solutions, formation of monovalent Cu^+ takes place during the simultaneous dissolution of the alloy [15]. The formed Cu^+ ion undergoes further oxidation to the more stable Cu^{2+} ion [16] according to:

$$Cu \rightarrow Cu^+ + e \quad (1)$$

$$Cu^+ \rightarrow Cu^{2+} + e \quad (2)$$

The corrosion reaction of the Cu alloys was described elsewhere [13]. The corrosion reaction of Cu–Al alloy can be represented by:

$$(Cu + Al) + 1/2(a+b)O_2 + 2(a+b)H^+ \rightarrow aCu^{2+} + bAl^{3+} + (a+b)H_2O \quad (3)$$

The cathodic counter part of this overall reaction is oxygen reduction which occurs in acidic solutions according to:

$$1/2(a+b)O_2 + 2(a+b)H^+ + 2(a+b)e^- \rightarrow (a+b)H_2O \quad (4)$$

In neutral or basic solution the reduction reaction leads to the formation of OH^-:

$$1/2(a+b)O_2 + (a+b)H_2O + 2(a+b)e^- \rightarrow 2(a+b)OH^- \quad (5)$$

The polarization resistance, R_p is related to the corrosion rate as corrosion current density, i_{corr}, according to the Stern-Geary Eq. [17]:

$$R_p \equiv \left(\frac{dE}{di}\right)_{i\rightarrow 0} \equiv \frac{\beta_a \beta_c}{2.3(\beta_a + \beta_c) i_{corr}} \quad (6)$$

where β_a and β_c are the anodic and cathodic Tafel slopes respectively. The calculated values of the cathodic Tafel slopes are relatively high, which indicates that the cathodic process is not controlled by charge transfer kinetics. The values of R_p and i_{corr} were calculated directly after reaching the steady state and are presented in Table 2. The corrosion current density was found to decrease with increase in the chloride concentration up to 0.15 M in the neutral 0.5 M Na_2SO_4 solution. For concentrations higher than 0.15 M a slight increase in the current density was observed. This behavior is attributed to the formation of an insoluble film that consists mainly of CuCl [18]. Above 0.15 M Cl^- (critical concentration), Cl^- ions attack the insoluble layer (CuCl) to form soluble complex of $CuCl_2^-$ which leads to the observed increase in the corrosion rate. The corrosion current density was found to change exponentially with chloride ion concentration. This means that log i_{corr} is a linear function of the concentration of Cl^- (cf. Fig. 3). The break point in the plot can be considered as the chloride concentration at which the insoluble layer of CuCl is attacked by Cl^- to form the soluble complex $CuCl_2^-$ [19, 20].

Table 2 Corrosion parameters for the Cu–Al alloy electrode immersed in neutral 0.5 M Na_2SO_4 as a function of chloride ion concentration

[Cl] (M)	E_{corr} (mV)	i_{corr} (μA cm^{-2})	β_a (mV $decade^{-1}$)	β_c (mV $decade^{-1}$)	R_p (kΩ cm^2)
0	–212	13.25	369	–498	6.9
0.01	–210	21.25	190	–529	2.8
0.05	–210	20.75	189	–588	2.9
0.075	–217	19	193	–485	3.2
0.1	–236	12	178	–428	4.5
0.15	–234	13	180	–359	4.0
0.25	–255	14.1	142	–362	3.1
0.3	–233	15.3	113	–390	2.5
0.35	–236	21.25	108	–406	2.0
0.45	–249	17.4	103	–388	2.0
0.50	–261	20.25	116	–371	1.9

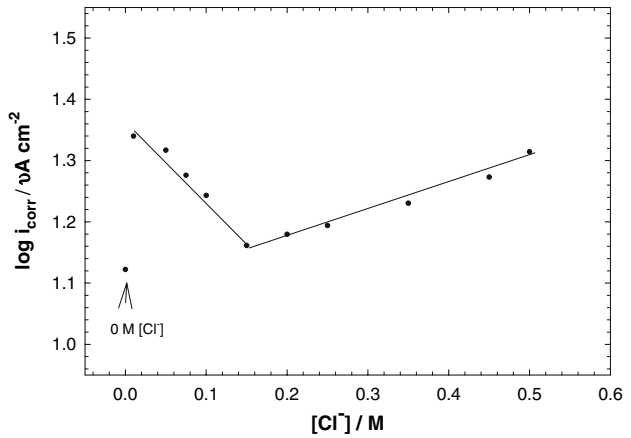

Fig. 3 Variation of log i_{corr} with $[Cl^-]$ for the Cu–Al alloy in neutral 0.5 M Na_2SO_4 solution, as a function of chloride ion concentrations at 25 °C

3.2.2 *Effect of temperature on the corrosion rate*

Since the working temperature of the heat exchanger tubes is always between 50 and 60 °C, it was essential to investigate the effect of temperature on the corrosion behavior of the alloy. For this reason the corrosion rate of the Cu–Al alloy, as the main working material of the heat exchanger, was investigated in naturally aerated 0.5 M Na_2SO_4 + 0.1 M NaCl solution at pH 7 in the temperature range 25–65 °C. The polarization values were analyzed and the calculated data are presented in Table 3. As expected, the rate of corrosion was found to increase with temperature. The relation between the corrosion rate presented as corrosion current density, i_{corr} and temperature was found to obey the familiar Arhenius Eq. [21]:

$$\frac{d \log i_{corr}}{d\frac{1}{T}} = -\frac{E_a}{R} \tag{7}$$

where, E_a is the molar activation energy of the corrosion process and R is the gas constant (8.314 J mol^{-1} K^{-1}). The Arhenius plot is presented in Fig. 4. The activation energy for the corrosion process was calculated and found to be ≈10 kJ mol^{-1}. This low activation energy value (<40 kJ mol^{-1}) is an indication that the dissolution (corrosion) process is under diffusion control [22–24].

3.2.3 *Potentiodynamic anodic polarization*

The electrochemical behavior of the Cu–Al alloy was investigated using potentiodynamic anodic polarization in 0.5 M Na_2SO_4 solution containing different chloride ion concentrations within the range of 0–0.5 M Cl^-. Typical data are presented in Fig. 5. Generally the anodic polarization curves exhibit a well defined anodic peak followed by a passive region then an abrupt increase in the anodic current at a critical potential value (E_b). At chloride concentration lower than 0.1 M, the value of E_b seems to be unaffected by the addition of chloride ions, whereas at chloride ion concentration from 0.1–0.5 M, the value of E_b is shifted to less positive values as the chloride ion concentration increases. Figure 6 presents the variation of E_b with the logarithm of chloride ion concentration. E_b varies linearly with the logarithm of $[Cl^-]$ according to the following relation [25]:

$$E_b = a - b \log[Cl^-] \tag{8}$$

where a and b are constants whose values depend on the scan rate [18]. The constant b represents the slope of the linear relationship and was calculated to be 239 mV. It represents the rate of decreasing of the break down potential with $[Cl^-]$. For other Cu alloys in neutral chloride solutions the constant b was 220 and 150 mV [9]. The three different values of (b) indicate its dependence on the type of electrode and the aggressiveness and aeration condition of the medium [9]. The anodic peaks shown in the polarization curves, (cf. Fig. 5), are attributed to the oxidation of copper to Cu (I) and further oxidation to Cu (II) [6, 7]. In chloride free sodium sulfate solutions the anodic peak is broad and extends over a potential range from 0.1 to 0.4 V and a maximum peak current of 50 mA cm^{-2} at about 0.3 V was recorded. Continuous addition of chloride ion was found to decrease the peak current up to a critical chloride ion concentration (≈0.15 M). Above this critical value the chloride ions attack the insoluble layer (CuCl) forming a soluble complex of $CuCl_2^-$ and the anodic current increases again.

3.2.4 *Potentiodynamic cyclic polarization*

The electrochemical behavior of the alloy under investigation was also studied by the potentiodynamic cyclic

Table 3 Corrosion parameters of Cu–Al alloy in 0.5 M Na_2SO_4 + 0.1 M NaCl solution at pH 7 at different temperatures

Temp. (°C)	E_{corr} (mV)	i_{corr} (μA cm^{-2})	β_a (mV $decade^{-1}$)	β_c (mV $decade^{-1}$)	R_p (kΩ cm^2)
25	–236	17	106	–205	1.78
35	–230	19	97	–182	1.40
45	–236	23.4	89	–192	1.12
55	–242	25.6	89	–173	0.99
65	–234	28.3	74	–189	0.813

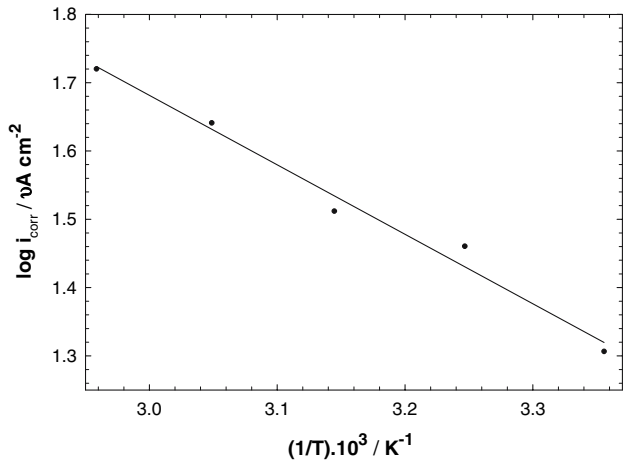

Fig. 4 Arrhenius plot (log i_{corr} vs. 1/T) of the Cu–Al alloy in neutral solution of 0.5 M Na_2SO_4 + 0.1 M NaCl

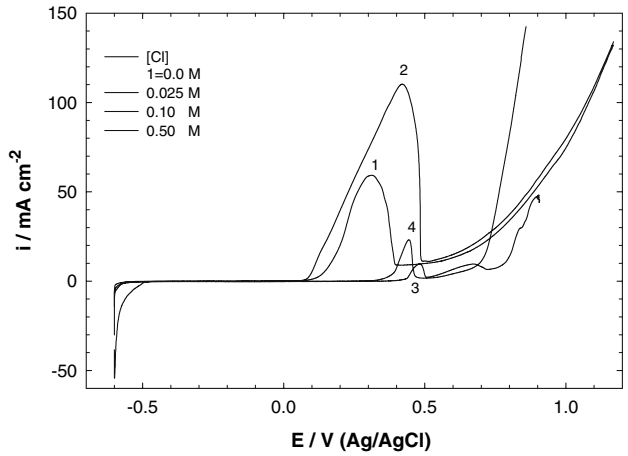

Fig. 5 Potentiodynamic polarization of the Cu–Al alloy in neutral solution of 0.5 M Na_2SO_4 solution containing different chloride ions concentrations at 25 °C and scan rate of 1 mV s^{-1}

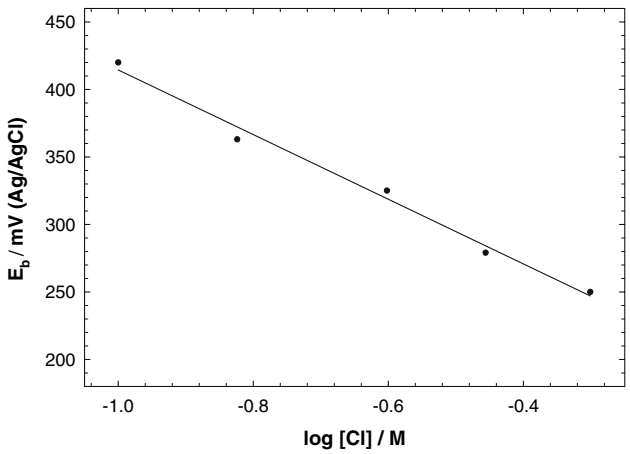

Fig. 6 Variation of E_b of the Cu–Al alloy with the chloride ion concentrations in neutral 0.5 M Na_2SO_4 solution at 25 °C and scan rate of 1 mV s^{-1}

polarization technique. The sulfate concentration was kept at 0.5 M and the chloride ion concentration was changed between 0.1 and 0.5 M. The results of these measurements are illustrated in Fig. 7. The potential scan started from –600 to 80 mV and then reversed in the cathodic direction with scan rate 5 mV s^{-1}. After commencing the potential scan at –0.6 V, low cathodic current is recorded, probably due to the formation of adsorbed species on the electrode surface according to the following scheme [18, 20, 26–28].

$$Cu + H_2O = Cu(H_2O)_{ads}$$

$$Cu + OH^- = Cu(OH)^-_{ads}$$

$$Cu + SO_4^{2-} = Cu(SO_4)^-_{ads}$$

$$Cu + Cl^- = Cu(Cl)^-_{ads}$$

The adsorption of anions on the anodized metal surface promotes dissolution or passivation with increasing potential [29]. The metal acquires a passive behavior due to the formation of an adsorbed layer [20, 30]. The adsorbed species represent an intermediate state for the active dissolution [8]. In the anodic active region, copper goes into the solution as Cu^+ ions [30, 31] and the current density is continuously increased with potential. The increase in the anodic current can be attributed to the dissolution of an adsorbed layer via Cu^+ ion formation as follows:

$$Cu(OH)^-_{ads} + OH^- = Cu(OH)^-_{2aq.} + e^-$$

$$2Cu(SO_4)^-_{ads} = Cu_2(SO_4)_{aq.} + SO_4^- + 2e^-$$

$$Cu(Cl)^-_{ads} + Cl^- = Cu(Cl)^-_{2aq.} + e^-$$

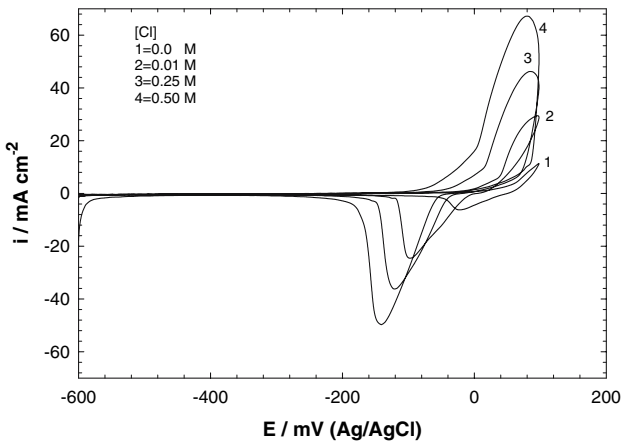

Fig. 7 Cyclic voltamogram of the Cu–Al alloy in neutral 0.5 M Na_2SO_4 solution as a function of chloride ion concentrations at 25 °C and scan rate of 5 mV s^{-1}

The potential scans in the negative direction show cathodic peaks which represents the reduction of copper ions to copper [3, 9]. The results indicate an increase in peak current for both the anodic and cathodic peaks with increase in chloride ion concentration, as seen in Fig. 8.

3.2.5 *The electrochemical impedance measurements*

The electrochemical impedance behavior of the Cu–Al alloy was recorded at different immersion times up to 120 min in 0.5 M Na_2SO_4 solution containing different concentrations of chloride ion [0.0–0.5 M]. Figure 9 represents the Bode plots recoded in 0.5 M Na_2SO_4 solution containing 0.5 M NaCl at pH 7. After longer immersion time (>5 min), the Bode plots show two phase maxima at intermediate and low frequencies. The absence of the impedance plateau and the presence of a second phase maximum at low frequency indicate that Warburg impedance is needed to explain this behavior [3, 32]. The initial impedance (Z) recorded after 5 min from electrode immersion drifts continuously upwards. The increase in the impedance value is due to progressive passive film formation until a steady state is achieved [28]. The impedance data were analyzed using software provided with the impedance system, where the dispersion formula was used. For a simple equivalent circuit model consisting of a parallel combination of a capacitance C_{dl} and a resistor R_{ct} in series with a resistor R_s, representing the solution resistance, the electrode impedance, Z, is represented by Eq. (10).

$$Z = R_s + \frac{R_{ct}}{1 + (2\pi f R_{ct} C_{dl})^{\alpha}} \tag{9}$$

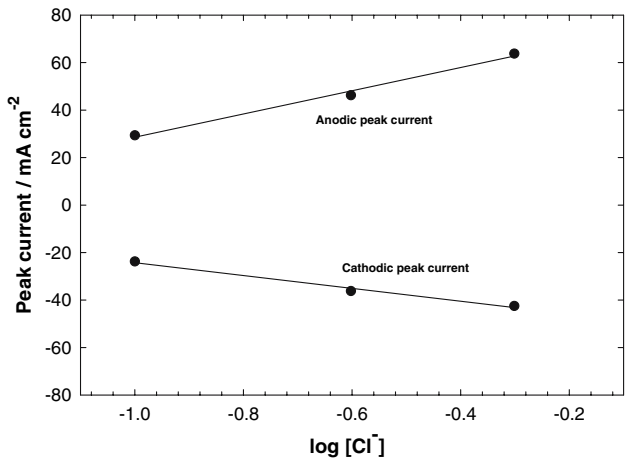

Fig. 8 Variation of the peak current of the Cu–Al alloy in neutral 0.5 M Na_2SO_4 as a function of chloride ion concentrations at 25 °C

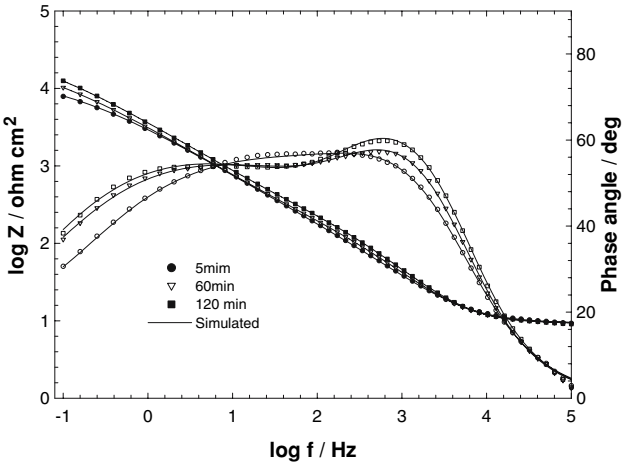

Fig. 9 Bode plots of the Cu–Al alloy immersed in neutral 0.5 M Na_2SO_4 solution containing 0.5 M NaCl as a function of immersion time at 25 °C

where α is an empirical parameter ($0 \leq \alpha \leq 1$) and f is the frequency in Hz. The above relation is known as the dispersion formula and takes into account the deviation from the ideal RC-behavior in terms of a distribution of time constant due to surface inhomogenties, roughness effects and variations in properties or compositions of surface film [33, 34]. To account for the diffusion process and surface film, the impedance data were analyzed using the equivalent circuit shown in Fig. 10, where another R_{pf}–C_{pf} combination and Warburg impedance (W) were introduced to account for the spontaneously formed passive film and the diffusion process, respectively. The diffusion process may indicate that the corrosion mechanism is controlled not only by a charge transfer process but also by diffusion [3]. The calculated equivalent circuit parameters are presented in Table 4. Figure 11 shows the variation of the resistance and the relative thickness of the passive layer in 0.5 M Na_2SO_4 + 0.5 M NaCl as a function of immersion time. Although the value of the relative thickness ($1/C_{pf}$) continuously decreases with time, the value of the resistance continuously increases. This indicates a change in the

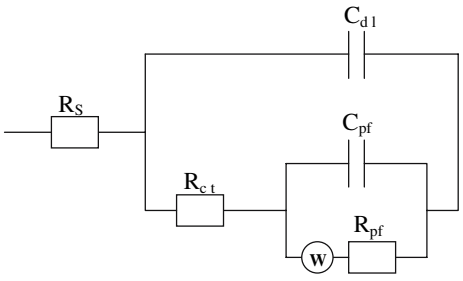

Fig. 10 Equivalent circuit: R_s = solution resistance, R_{ct} = charge transfer resistance, C_{dl} = double layer capacitance, R_{pf} = passive film resistance, C_{pf} = passive film resistance, W = Warburg impedance

Table 4 Equivalent circuit parameters of the Cu–Al alloy immersed in 0.5 M Na_2SO_4 solution containing different chloride ion concentrations at pH 7 as a function of immersion time

[Cl^-] (M)	Time (min.)	R_s (Ω)	C_{dl} (μF cm^{-2})	α_1	C_{pf} (μF cm^{-2})	α_2	R_{ct} (Ω cm^2)	R_p (kΩ cm^2)	W (kΩ $s^{-1/2}$)
0	5	18.70	25.8	0.70	18.2	0.70	83.0	1.38	2.266
	60	19.38	16.6	0.80	15.6	0.73	631.0	2.05	19.000
	120	18.99	15.9	0.80	13.5	0.80	718.0	2.00	23.800
0.05	5	18.17	38.0	0.80	15.2	0.60	48.2	1.80	2.686
	60	18.28	34.4	0.80	14	0.60	75.0	2.43	4.317
	120	18.35	31.6	0.81	12.4	0.60	88.0	2.24	4.983
0.1	5	17.11	25.9	0.80	13.1	0.60	42.8	2.65	2.965
	60	17.00	30.7	0.83	13.2	0.60	53.6	3.80	5.500‘
	120	16.92	31.2	0.85	12.7	0.60	60.5	3.38	5.985
0.15	5	12.3	31.3	0.80	8.6	0.60	104	1.00	2.452
	60	12.63	32.6	0.83	13.7	0.60	71.7	2.16	2.322
	120	12.52	31.7	0.83	14.0	0.60	70.0	2.55	2.713
0.25	5	13.5	40.4	0.80	12.0	0.60	45.7	1.20	2.284
	60	17.8	41.1	0.80	23.0	0.60	42.2	2.30	1.602
	120	11.2	38.5	0.84	24.8	0.60	40.0	2.70	1.700
0.35	5	12.55	62.2	0.80	21.0	0.60	35.0	1.33	1.536
	60	12.5	56.2	0.82	27.5	0.60	31.0	1.80	2.392
	120	12.4	50.4	0.84	28.3	0.60	33.3	2.20	2.671
0.5	5	10.4	52.6	0.82	21.7	0.60	14.6	1.00	1.500
	60	10.4	48.7	0.85	33.9	0.62	20.6	1.55	1.400
	120	10.2	44.7	0.86	36.5	0.70	29.1	1.68	2.600

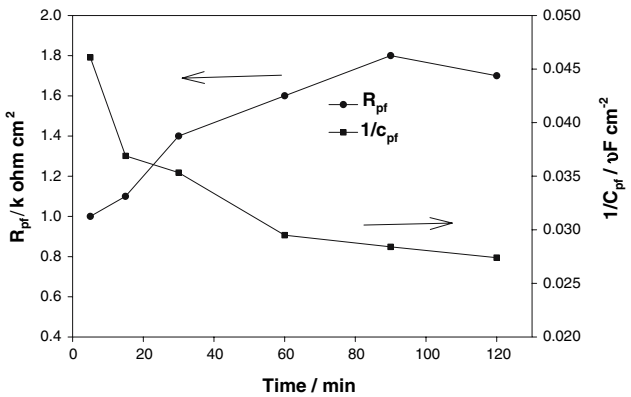

Fig. 11 Variation of the resistance and relative thickness of the passive layer on the Cu–Al alloy in neutral 0.5 M Na_2SO_4 solution containing 0.5 M NaCl as a function of the time of electrode immersion in the electrolyte

passive film structure and/or composition. In this respect, the passive film can be represented by a duplex layer [13, 24]. The first is a relatively thick porous outer layer on the top of the second, which is thin and compact passive layer. The lower value of α (0.6) indicates the presence of a diffusion process at the interface [3]. This diffusion process may indicate reversible dissolution which is accompanied by the formation of a porous film. It is an indication of the formation of a passive film via a dissolution–precipitation mechanism under open-circuit conditions [20, 32]. The variation of the passive film resistance, R_{pf} and its relative thickness $1/C_{pf}$, after 120 min immersion time in 0.5 M Na_2SO_4 containing different chloride ion concentrations is presented in Fig. 12. Addition of [0.05–0.1M] Cl^- leads to a slight increase in R_{pf} without affecting the film thickness. This can be attributed to the presence of an insoluble CuCl layer. Above a critical value [Cl^-] ≥ 0.1 M, both R_{pf} and the film thickness decrease with increasing chloride ion concentration on the alloy surface due to the formation of the soluble complex [$CuCl_2^-$].

4 Conclusions

Addition of a low concentration of Cl^-, ([Cl^-] <0.15 M) to Na_2SO_4 solution used in the extraction of Na_2SO_4 from Quaron Lake decreases the corrosion rate due to the formation of an insoluble layer of CuCl. At higher concentration of chloride ion (>0.15 M), the corrosion rate increases due to the formation of soluble complex $CuCl_2^-$ and the corrosion current density changes exponentially with [Cl^-]. The activation energy of the corrosion process was found to be 10 kJ mol^{-1}. This value indicates that the dissolution (corrosion) process is under diffusion control.

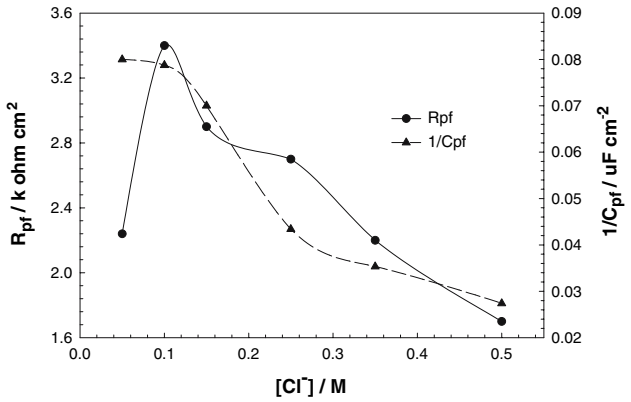

Fig. 12 Variation of the resistance and the relative thickness of the passive film on the Cu–Al alloy as a function of [Cl^-] in neutral 0.5 M Na_2SO_4 solution at 25 °C

The passive film formed on the alloy surface consists of an outer porous relatively thick layer on the top of a very thin compact layer. It is recommended that the solution mixture for the production of sodium sulfate consists of 0.5 M sodium sulfate +0.15 M sodium chloride at pH 7.

References

1. Cahn RW, Hassen P, Kramer ES (1996) Material science and technology, a comprehensive treatment, vol 8. Structure and properties of non-ferrous alloys. VCH, New York
2. Kear G, Barker BD, Stokes K, Walsh FC (2004) J Appl Electrochem 34:659
3. El-Sherif RM, Ismail KM, Badawy WA (2004) Electrochim Acta 49:5139
4. Ismail KM, Fathi AM, Badawy WA (2004) J Appl Electrochem 34:823
5. Kear G, Barker BD, Stokes K, Walsh FC (2004) J Appl Electorchem 34:1241
6. Schussler A, Exner HE (1993) Corros Sci 34:1793
7. Schussler A, Exner HE (1993) Corros Sci 34:1803
8. Scully JC (1990) The fundamentals of corrosion. Pergamon Press, Oxford
9. Barbucci A, Farne G, Matheazzi P, Riccieri R, Cerisola G (1990) Corros Sci 41:463
10. El-Egamy SS, Badawy WA, Shebata HS (2000) Corros Prev Control 47:35
11. El-Egamy SS, Badawy WA, Shebata HS (2001) Materwiss Werksttechnick 31:737
12. El-Egamy SS, Badawy WA (2004) J Appl Electrochem 34:1153
13. Badawy WA, Al-Kharafi FM, El-Azab AS (1998) Curr Top Electrochem 6:149
14. Man HC, Gabe DR(1981) Corros Sci 21:323
15. Badawy WA, Al-Kharafi FM (1997) Bull Electrochem 13:392
16. Al-kharafi FM, Badawy WA (1997) Electochim Acta 42:579
17. Stern M, Geary AL (1957) J Electrochem Soc 104:56
18. Dechialvo MRG, Salvarezza RC, Vasquez Moll D, Arvia AJ (1985) Electrochim Acta 30:1501
19. Lal H, Thirsk HR (1953) J Chem Soc Part III:2638
20. Ismail KM, El-Egamy SS, Abd El-fatah M (2001) J Appl Electrochem 31:663
21. Atkins PW (1994) Physical chemistry, 5th edn. Oxford University Press, Oxford, p 877
22. Wieckowski A, Ghali E (1985) Electrochim Acta 30:1423
23. Wright GA (1967) J Electrochem Soc 14:1263
24. Al Kharafi FM, Badawy WA (1998) Corrosion 54:377
25. Lekie HP, Uhlig HH (1961) J Electrochem Soc 108:209
26. Al-kharafi FM, El-Tantawy YA (1982) Corros Sci 22:1
27. Rice-Jackson LM, Horanyi g, Wiekowski A (1991) Electrochim Acta 36:753
28. Ismail KM, Fathi AM, Badawy WA (2004) Corros Sci 60:795
29. Parkhutik VP, Albella JM, Martinez-Duart JM (1992) Electric breakdown in anodic oxide films. In: Conway BE, Bockris JM, White RE (eds) Modern aspects of electrochemistry, vol 23. Plenum Press, New York, p 330)
30. Jardy A, Legal Lasalle-Molin A, Keddam M, Takenouti H (1992) Electrochim Acta 37:2195
31. Ismail KM, Badawy WA (2000) J Appl Electrochem 30:1303
32. Strehblow HH, Titze B (1980) Electrochim Acta 25:839
33. Hladky K, Colow LM, Dawson JC (1980) Br Corros J 15:20
34. Hitzig J, Titze J, Juettner K, Lorenz WJ, Schmidt E (1984) Electrochim Acta 29:284